Nuclear stopping in polycrystalline materials: Range distributions and Doppler-shift attenuation analysis

M. Hautala
Department of Physics, University of Helsinki, Siltavuorenpenger 20D, SF-00170 Helsinki 17, Finland
(Received 27 February 1984; revised manuscript received 21 May 1984)

We describe a comprehensive computer program COSIPO, computer simulation in polycrystals, which uses the binary-collision approximation to simulate the slowing down of heavy ions in the keV region in crystalline targets. The atomic scattering is governed by a potential which is chosen as an option. Inelastic losses are either impact-parameter-dependent or friction type. Thermal vibrations of the target atoms can be included. Various ways to treat polycrystallinity are described. The range distributions are compared with results based on existing codes and the significance of various parameters is studied. The effect of crystalline structure on the results of Doppler-shift attenuation measurements [line shapes and $F(\tau)$ values] is calculated in various ways. Both range distributions and line shapes are found to be in agreement with experiment. Nuclear stopping during the slowing-down process in polycrystalline materials can be either smaller or larger than in amorphous materials. Some possible applications of the results are discussed.

I. INTRODUCTION

In recent years considerable progress has been made in calculating the potential between colliding atoms and hence in calculating the nuclear stopping power of low-energy ions in amorphous solids. Wilson and Bisson[1] used a modified Wedepohl method[2] originating from Gombas[3] to calculate the potential between closed-shell atoms. In this method the charge distributions of the individual atoms are calculated using the Hartree-Fock-Slater formalism. When the interaction energy of the colliding atoms is calculated, the charge distributions are assumed to be undisturbed. The total energy of interaction between the two charge distributions is calculated from the Coulomb, kinetic, and exchange energies. Wilson *et al.*[4] found these potentials to be suitable for the calculation of nuclear stopping.

We have calculated[5] the potentials by using Dirac-Fock (DF) electron distributions in the original Gordon-Kim method,[6] in which a small correlation term is included. We have tested the potentials by comparing with experiment the calculated ranges and range distributions of several ions in various amorphous materials and found them to agree to within 10% over the reduced energy interval $\epsilon \approx 0.1-1$ (Refs. 5 and 7–9). The potential is tested in these calculations to less than $10a_{\mathrm{LSS}}$ [the Lindhard-Scharff-Schiøtt radius $a_{\mathrm{LSS}}=0.8852a_B/(Z_1^{2/3}+Z_2^{2/3})^{1/2}$, $a_B=0.529$ Å]. Recently, we studied the multiple scattering of several 50-keV ions in xenon targets.[10] In comparing the widths of lateral distributions with experiment, the potentials were tested up to $20a_{\mathrm{LSS}}$.[10] Even in this case reasonable agreement was achieved. However, when the experimental targets were polycrystalline, the calculations assuming amorphous targets are quite inadequate, especially in reproducing the tails of the distributions (e.g., Refs. 11–13). For example, the experimentally measured range of 60-keV Al in Ta is larger than the calculated one by a factor of 1.47 ± 0.06.[12]

In the analysis of Doppler-shift attenuation (DSA) measurements at low reduced-recoil energies ($\epsilon \sim 0.1-1$), the problem of not knowing the slowing down in polycrystalline materials has been overcome by using experimental correction factors for nuclear (f_n) and electronic (f_e) stopping powers and by assuming the material to be amorphous. Since the lifetimes and line shapes of the emitted γ rays are sensitive to the stopping value of the recoiling atom, the correction procedure is both possible and obligatory. The actual procedure in determining constant f_n and f_e values has been typically carried out by fitting calculated and experimental mean ranges and line shapes at 0° and 90° detector angles.[11] Typical values for the dominant f_n values have been 0.7–0.8. Although the procedure has been found to be successful, it is still not known how the polycrystalline structure affects the line shapes and $F(\tau)$ values, or how well f_n and f_e are energy independent. The consequence of using an average correction for the stopping (so that the average slowing down should be correct) is seen when we compare the range distributions. As a result of using f_n values (e.g., 0.7) the modal range is shifted away from the experimental value by about the same amount. However, the experimentally determined tails cannot be reproduced, which leaves the possibility that some diffusion phenomenon is the origin of the tails.[9] An uncertainty is therefore introduced into the correction values. The fact that surface peaks are often found in the implanted profiles indicates some diffusion tendency.[12,13]

Two methods have been used for simulations of the slowing down of energetic ions in crystalline solids. In the first case the force equations are solved by taking into account the n-body interactions [multiple-interaction method (MIM)] (e.g., Refs. 14–16). This method is more applicable at low energies, where n-body events are important; at higher energies the computing time required precludes its use. This method is also generally restricted to studies where statistical information is unnecessary. The

other method, the so-called binary-collision—approximation method (BCAM) is superior at high energies because of its rapidity. Robinson and Oen used this latter method in the 1960s to study in detail the common features of the slowing down of energetic ions in various crystals.[17] In the 1970s the code was extended (and named MARLOWE) to treat displacement cascades,[18] and later still, an improved method was developed for simultaneous collisions.[19] MARLOWE has primarily been used to treat fusion-reactor, first-wall problems, i.e., sputtering, reflection, and radiation damage, and for light particles at low energies. In recent reviews Harrison[20] and Robinson[21] have discussed the limitations of each of these methods in detail, especially in the case of sputtering.

There has been a limited amount of interest in studying in detail the fundamentals of the stopping problem, i.e., the accuracy of the nuclear stopping in crystalline materials. In the 1960s, when channeling was discovered by Robinson and Oen using simulation[17] and was confirmed experimentally, the comparison between theory and experiment was only qualitative because there were too many unknown factors (see Ref. 22). In particular, the potential was uncertain. The situation has now changed, since our knowledge of the potential has improved considerably. Nevertheless, there is still the need to know better the stopping power in polycrystalline materials, because of their common usage in experiment.

In addition, the results of the MIM and BCAM seem to be somewhat contradictory.[23] It thus seemed useful to construct an independent code specially designed for studies of range distributions and the analysis of DSA measurements in polycrystalline materials, where statistical information is needed, in the keV region. The simultaneous collisions are then less important and BCAM is adequate, so that we can concentrate on the speed of the program.

The aim of this paper is to describe the new computer code COSIPO (computer simulation in polycrystals), and to study its accuracy and the significance of the approximations. We also want to compare these results with the results of the other codes and try to understand any differences that might occur. Some results of the analysis of the DSA measurements are given and possibilities of applying the method in new areas are described. Finally, and most importantly, we attempt to provide a comprehensive overview of our understanding of nuclear stopping, both in the range and DSA measurements in polycrystalline materials. We will show that the *structure* of the material is of significance to the "effective" nuclear stopping during the slowing-down process, which can be *smaller* or *larger* than in an amorphous material.

II. PROCEDURE

A primary aim in developing the code COSIPO was to make a code as fast as possible without any serious loss of accuracy, with a view to its use in the slowing down of heavy ions in the keV region in polycrystals. In order to check the accuracy of some of the approximations and to compare the results with other calculations, various options were set up in the code.

A. Collisions

The scattering is calculated in the binary-collision approximation. The following possibilities are used in the present work for determination of the scatterer, from the nearest and next-nearest neighbors, and in the determination of simultaneous collisions.

(i) SCA1. The scatterer is the target atom with the smallest impact parameter. This is a fast method intended especially for polycrystalline targets.

(ii) SCA2. The scatterer is the atom which is nearest and which has an impact parameter less than $b_{\max}$, which may be a constant or may be determined by a specified scattering angle. However, if there is a scatterer that has a smaller impact parameter at a distance which deviates by less than $x_{\min}$ from the nearest neighbor, that scatterer is chosen. If the distances to some other target atoms deviate by less than $x_{\min}$ and the impact parameters are less than $b_{\max}$, the collisions with those target atoms are treated simultaneously. The final direction of the ion after the simultaneous collisions is determined by adding the momenta vectorially. In all the distributions presented, $b_{\max}=2.0$ Å and $x_{\min}=0.4$ Å, unless otherwise stated. More involved methods exist,[19] but this method has been found to be adequate for the present purposes; i.e., the importance of simultaneous collisions can be studied by varying $b_{\max}$. If the results are sensitive to $b_{\max}$, the BCA method is in any case inaccurate, and the MIM should be used. Some care must be exercised when choosing $b_{\max}$, because too large $b_{\max}$ values may sometimes lead to neglect of the nearest collisions, as only the nearest and next-nearest neighbors are included in the search for the next scatterer.

B. Potential and scattering angle

When the method described in the Introduction is used to calculate a potential,[5] a different potential for each pair of atoms is obtained, thus making the calculation unwieldy. Therefore we calculated a mean of the potentials in reduced units, a_{LSS}, which is a good approximation for the individual potentials at not too small energies.[5] Somewhat better agreement was possible by introducing a new scaling parameter $a'=a_{\mathrm{LSS}}[\alpha+\beta(Z_1+Z_2)^{\gamma}]$.[5] Ziegler *et al.* later used a similar method.[24] In the following, either an individual (=DF) or the mean (=MEAN) potential[5] in a_{LSS} units is used when making comparison with experimental range distributions. When the reduced energy ϵ is of the order of 1, there is little difference in the stopping calculated from the various potentials.[5,25]

The potential between atoms in a solid is different from that between undisturbed atoms at greater distances. In metals we may consider that the zero of the potential energy is changed. The change may be naturally included in MI simulations. In the BCA calculations the change may be studied by suitable "erosion" of the potential, i.e., by subtracting a constant from the potential energy so that it goes to zero, e.g., in the middle of the channel. This reduces the energy loss, but keeps the force at zero in the middle of the channel. The potential can also be *truncat-*

ed, i.e., it is set to zero after a definite distance, whereas at shorter distances there is no change in the potential.

In order to compare the present program with other methods, some other potentials are also used, as we show in the following.

For Cu-Cu, the Born-Mayer (=BM1; see Ref. 17),

$$V_{\mathrm{BM1}}(r)=(22.5\ \mathrm{keV})\exp(-r/0.1966\ \text{Å})\ ,$$

or the Born-Mayer—plus—Bohr (=BMB; see Ref. 15) potentials is used,

$$V_{\mathrm{BMB}}(r)=V_{\mathrm{BM1}}(r)+(12/r\ \mathrm{keV})\exp(-r/0.12\ \text{Å})\ ,$$

for Xe-W, the Born-Mayer (=BM2; see Ref. 26) potential is used,

$$V_{\mathrm{BM2}}(r)=(80.8\ \mathrm{keV})\exp[-4.75r\ (\text{Å})]\ ,$$

and for D-Ni, the Thomas-Fermi-Moliere (TFM) potential is used. In the DSA calculations, where the potential is rather irrelevant, the commonly used Thomas-Fermi (TF) potential is taken.

The scattering angle (and the time integral) is evaluated from the standard scattering integral[18] using the transformation suggested by Latta and Scanlon.[28] The integrals are calculated either by the Simpson method or the n-point Gaussian-Mehler quadrature. In the beginning of the simulation, 5000 scattering angles and time integrals for 100 impact parameters and 50 energies are calculated and stored in a look-up table for later use. The axes of the table are either both logarithmic, or energy is logarithmic while impact parameter is linear; the choice depends on the relative importance of small or large impact parameters. The different possibilities are for checking purposes. The interpolated angle deviates less than 1% from the exact value. Instead of using the look-up table, it is also possible to calculate the integral explicitly (e.g., when the potential is discontinuous or in test runs).

C. Thermal vibrations

Thermal vibrations are included by assuming the displacements to be uncorrelated and Gaussian-distributed. For later use, 1000 displacements for 1000 random numbers are stored in a look-up table. The displacements in the x, y, and z directions are calculated independently. The mean-square displacement is based on the Debye model, the only parameters required being the temperature and the Debye temperature Θ_D.

D. Inelastic energy loss

The following choices are used in the present calculations.

(i) LSS: A viscous force according to the LSS theory ($dE/dx=-kE^{1/2}$).[29]

(ii) Firsov: Impact-parameter dependent, according to the Firsov theory,[30] including all scatterers for which the impact parameter is less than a parameter called $EL_{\max}$. ($EL_{\max}=2.0$ Å in the present calculations.)

In each case it is possible to use a correction factor f_e. If needed, it would be possible to use more refined methods in the calculations for dealing with inelastic scattering. In the present calculations the electronic energy loss is of minor importance, and any associated inaccuracy would not affect our conclusions. By varying the parameters f_e and $EL_{\max}$ it is easy to study the importance of the electronic stopping.

E. Target structure

1. Polycrystalline target

a. Poly1. The direction of the beam is isotropic and the fixed crystal orientation determines the coordinate axis. The azimuthal angle ϕ is $\phi=2\pi P_1$ and the polar angle θ is $\theta=\arccos(1-2P_2)$, where P_1 and P_2 $(0<P_1,\ P_2<1)$ are random numbers. Robinson and Oen[17] called the calculation *isotropic,* when the primaries originate at lattice sites, i.e., $x=y=z=0$. This way of calculation, however, is not satisfactory, because of the unique nature of the lattice site.

A problem arises if the distributions of positions are required also to be uniform over the symmetry element of a particular crystallographic surface. Let the symmetry element be $-a/2<x,y\leq a/2$, where a is the lattice constant. Then, if $\theta=\pi/2$, there is a head-on collision without any dependence on ϕ. This occurrence should be very rare. As the area seen by the beam is relative to $\cos\theta$, the probability density for the angle θ to be between $\theta,\theta+d\theta$ is $\sin\theta\cos\theta\,d\theta$. From this it follows that θ can be calculated from

$$\theta=\tfrac{1}{2}\arccos\{\cos(2\theta_{\min})-[\cos(2\theta_{\min})-\cos(2\theta_{\max})]P\}\ ,$$

where $\theta_{\min}$ and $\theta_{\max}$ are the minimum and maximum of the polar angle, respectively. This method is particularly suitable if the microcrystals tend to orient in some direction, i.e., if there is texture. If there is no texture, $\theta_{\min}=0°$ and $\theta_{\max}=90°$.

b. Poly2. The direction of the beam is fixed and the crystal is rotated (or actually the coordinate system). The random orientation of the crystal is achieved as follows: First, the direction of the new z axis is chosen randomly and then the x and y axes are randomly rotated around this new z axis. The "isotropic" calculation again follows, if the primary originates at $x=y=z=0$. The problem now arises how to choose the initial position of the primaries at the surface, because the axes of the crystal do not coincide with the laboratory coordinates. We have solved the problem simply by choosing $-100a<x,y<100a$ randomly and then searching for the nearest target atom. Although the positions are not chosen from a perfect symmetry element, the large area taken ensures that the error is small. The two methods are always found to yield very similar results. When the target is *polycrystalline* (calculated by either the Poly1 or Poly2 method), each grain is assumed to be infinitely thick.

2. Other possibilities for target structure

Instead of random rotation, it is possible to rotate the crystal or beam direction between specified θ angles and

thus simulate the *texture* of the target. If the crystal is rotated randomly between collisions the target is referred to as "*random*."

It is also possible to use the more specified targets needed especially in the DSA analysis. The crystal may in the beginning be rotated randomly and later have texture, or it may initially have texture and then be randomly rotated after some specified number of collisions, thus stimulating *damage* and implanted atoms. A slightly modified version includes also the implanted atoms in the crystalline structure. Some comparisons are made with Monte Carlo simulations in an *amorphous* material. For an explanation of these simulations the reader is referred to Refs. 5 and 9.

F. DSA analysis

As an option, the code also includes the DSA analysis, the calculation of $F(\tau)$ values, and line shapes of γ-rays. Each particle represents a specified number (five in the present calculations) of lifetime values τ, and for each τ value a definite number of γ's are emitted. The actual emission time T for each γ ray is obtained by $T=-\tau\ln(P)$, where τ is the mean lifetime of the level. For an explanation of the DSA-analysis method and of its underlying concepts, the reader is referred to Ref. 31, where a Monte Carlo method for DSA analysis, using the LSS differential cross section[29] for collisions and an amorphous target, is described in detail. This analysis method has proved successful, provided that f_n- and f_e-correction factors for stopping are used. These can be experimentally determined.[11]

A statistical error for a $F(\tau)$ value is calculated in the following way. The $F_\gamma(\tau)$ values for each γ ray are combined into a histogram of 100 channels $(n_1, \ldots, n_{100})$, the mean of the $F_\gamma(\tau)$'s being $F(\tau)$. The number of $F_\gamma(\tau)$ values in each channel is assumed to be Gaussian-distributed with a mean n_i and a standard deviation $(n_i)^{1/2}$. For each channel a random number is generated, which determines the actual n_i for that channel. In this way a new $F_j(\tau)$ can be calculated. This procedure is repeated 100 times. The standard deviation of these 100 $F_j(\tau)$'s is then the error of $F(\tau)$. Although five $F_\gamma(\tau)$'s per τ value per ion are calculated, and therefore the $F_\gamma(\tau)$'s are not properly uncorrelated, the method should give a reasonable estimation of the reliability of the calculated $F(\tau)$ value.

III. CALCULATIONS

A. Comparison with other codes

Harrison *et al.*[23] found large differences between the BCAM (truncated BM1 potential) and MIM (BM1 potential) in the case of 5-keV Cu in ⟨110⟩ Cu. Therefore we have chosen this case for comparison. The BCA and MI results taken from Ref. 23 are presented in Fig. 1 together with distributions from COSIPO. It is seen that, when the SCA2 method is used, the BCAM result is reached by the truncated BM1 potential and the MIM curve is approximately found by the BM1 potential. This shows that the

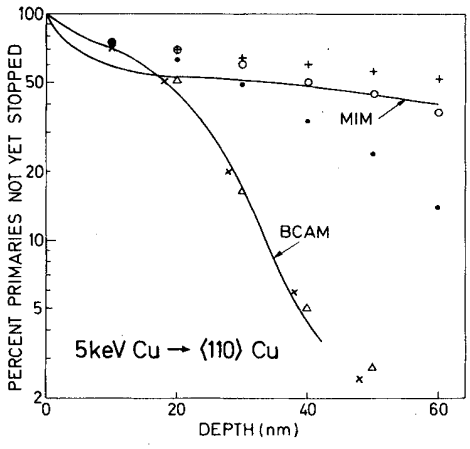

FIG. 1. Integral penetration distributions for 5-keV Cu in ⟨110⟩ Cu. BCAM, the binary-collision simulation of Robinson and Oen (Ref. 17), the potential being truncated BM1, and MIM, the multiple interaction simulation of Harrison *et al.* (Ref. 23) with the potential BM1, are compared with the present simulations with truncated BM1 and the SCA1 (△) or SCA2 (×) method, and BM1 with the SCA1 (●) and SCA2 (○) method. + refers to the calculation in which the BM1 "eroded" potential with SCA2 was used. The truncated and "eroded" potentials were cut at 1.278 Å. The inelastic energy loss has been omitted in all the calculations.

difference is due mainly to truncating the potential at 1.278 Å. On the other hand, the SCA1 results show that it is important to take into account the simultaneous collisions when the BM1 potential is used. For this potential, focusing is effective.

The general agreement with the MIM can be improved by "eroding" the potential. The different absolute values can probably be associated with the computational problems in the MIM in determining the "effective representative area" in which ions actually remain long enough to be counted.[26] One should remember that a static lattice is assumed and no electronic stopping was included, thus enlarging the effect of the potential. In reality the differences between the the different methods are not as large as in Fig. 1.

A comparison with another MI code of Lutz *et al.*[15] is presented in Fig. 2 in the case of 20-keV Cu in ⟨111⟩ Cu. These workers included LSS electronic stopping and took the six nearest neighbors into account in the calculations. Again, good qualitative agreement using expected parameters can be found. The distance from the middle of a channel to the three nearest atoms is 0.74, 1.28, and 1.95 Å, thus limiting the $b_{\max}$ value.

A third comparison with the MIM is given in Fig. 3, where the 5-keV Xe atom in the ⟨100⟩ W case is studied. In this case the results are in quantitative agreement. The rms vibration amplitude differs from the experimental one (0.049 Å) because of the erroneous formula used in Ref. 26 (the integration limit in the equation for the rms displacement should be Θ/T and not T/Θ). In Fig. 3 the experimental curve is also presented, which indicates that the BM2 potential is too strong.

The 5-keV Xe atom in the ⟨100⟩ W case is studied fur-

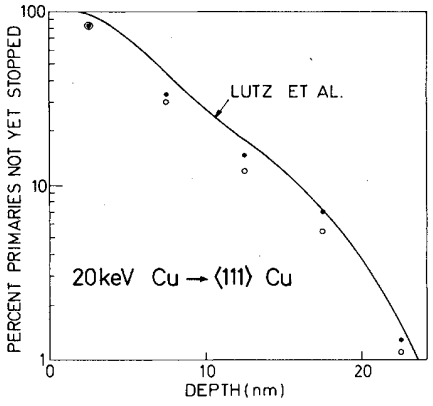

FIG. 2. Integral penetration distributions for 20-keV Cu in ⟨111⟩ Cu using the BMB potential. The MIM calculation of Lutz *et al.* is reproduced from Ref. 15. In the present simulations both SCA1 (●) and SCA2 (○) methods were used with $b_{max}=1.5$ Å.

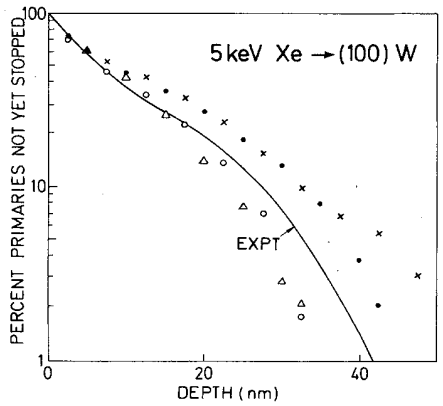

FIG. 4. Integral range distributions of 5-keV Xe in ⟨100⟩ W. The experimental curve is reproduced from Ref. 27. When the SCA1 method was used, the potential was DF-eroded (△). With the SCA2 method, the DF potential was either eroded (●) or not eroded; in the latter case, b_{max} was either 1.58 (○) or 2.0 Å (×).

ther in Fig. 4 using the DF potential and an experimental correction factor $f_e=1.6$ (Ref. 32) for Firsov electronic stopping. The distribution is sensitive to the potential and computational details, indicating that simultaneous collisions are important in this case; with expected parameters, however, good agreement with experiment can be found. It can be seen that the SCA1 method with an "eroded" potential is still a rather good approximation in this energy range (reduced energy $\epsilon\simeq 4\times 10^{-3}$). This example shows that, in principle, low-energy channeling experiments can be used in the determination of potential parameters, although the treatment of simultaneous collisions may cause problems. The MIM would be superior for these types of calculations. We have, in an earlier paper,[33] compared the simulations with experiment as a function of crystal orientation, energy, and temperature in more detail. At higher energies, where the calculations are not so sensitive to the parameters, the experimental problems became evident.

Finally, comparison with MARLOWE is presented in Fig. 5 for the case of 10-keV D in polycrystalline Ni.[34] The simulation of a single particle's history required over 1000 collisions, the movement of D-atoms being diffusionlike. Test runs showed that identical initial conditions yielded widely varying final positions, indicating diffusional movement and lack of accuracy in the calculations,

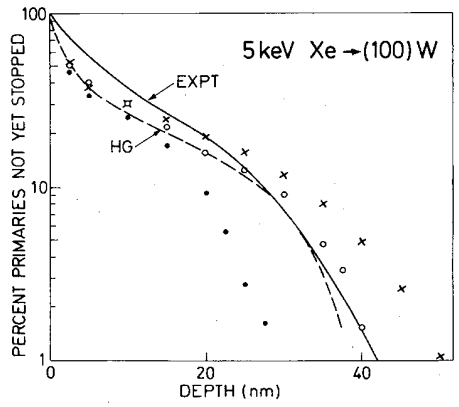

FIG. 3. Comparison of the previously calculated (Ref. 26) (HG) and experimental (Ref. 27) range distributions with the present simulations for 5-keV Xe in ⟨100⟩ W. In the calculations either the "eroded" BM2 potential and SCA1 is used (×), or the BM2 potential and SCA2 with b_{max} either 1.5 (●) or 2.0 Å (○). The electronic stopping was LSS with $f_e=0.25$, and the rms vibration amplitude was 0.022 Å.

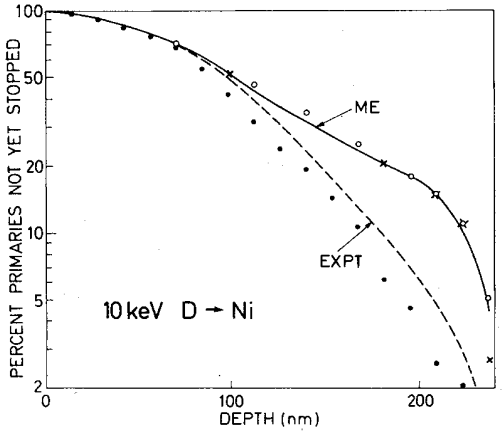

FIG. 5. Integral range distributions of 10-keV D in polycrystalline Ni. The experimental curve is reproduced from Ref. 34. The solid curve is the MARLOWE simulation of Möller and Eckstein (Ref. 34) assuming a static lattice, Thomas-Fermi-Moliere (TFM) potential, and LSS electronic stopping with $f_e=1.086$. The present results with the same assumptions are the following: ×, SCA2 method, $b_{max}=d_{max}=1.5$ Å, ○, SCA1 method, eroded TFM potential. Also presented are the results including thermal vibrations (the rms vibration amplitude is 0.059 Å) at room temperature, assuming a polycrystalline lattice (●).

whereas the distributions from separate runs were in agreement with each other. Thus our simulations should be also reliable in this extreme case, and comparison with the MARLOWE result shows good agreement. Also, the SCA1 method, being 40% faster than SCA2 in this case, yields the correct result. Möller and Eckstein did not include thermal vibrations in their simulations and they had to add some damage to the crystal in order to achieve the experimental result.[34] As Fig. 5 shows, if the vibrations are included, the theoretical curve lies below the experimental curve and instead of introducing damage we must look for some other remedy. We found a similar phenomenon also in the case of 120-keV Pb in Al and 60-keV Al in Ta,[35] where experimentally measured profiles[11,12] could be reproduced if noticeable texture was included. In the present case the difference might also be due to the importance of the correlations in the vibrations.[36] The effect of correlations on the relative vibration of an atom is to make the standard deviation of its distribution smaller. Using the rms value 0.046 Å, the experimental curve could be reproduced.

B. DSA analysis

It is clear that to explain away the tails in the range distributions by texture is only one possibility and that diffusion phenomena[37] could also cause tails. It has been pointed out that experimental range profiles may be obtained in this latter way.[9] Therefore some additional information is needed to determine the correct physical explanation. The results of the (p,γ) DSA measurements depend strongly on stopping conditions, but not on diffusion, and therefore could yield some information. In the following we compare both experimental range distributions and DSA-measurement results with simulations.

In an earlier paper we have shown, for the case of 60-keV Al in Ta, that the distributions are sensitive to thermal vibrations and the texture, but are less dependent on the potential or on the inelastic energy loss.[38] Further tests show that the results in this energy region ($\epsilon \sim 0.1-1$) are not sensitive to the various parameters when polycrystalline targets are treated, and especially that the SCA1 method, together with the TF potential, is sufficiently accurate. This is the method that is used in all the simulations presented in the following for 60-keV ^{22}Ne range distributions in Mo and for the DSA analysis in the reaction ^{22}Ne$(p,\gamma)^{23}$Na, $E_p = 1005$ keV, in Mo. These present a good basis for a direct test, because they have recently been thoroughly studied experimentally as a function of fluence.[39] When the TF potential was used in the analysis and amorphous backing assumed, correction factors of $f_n = 0.78$ and $f_e = 1.0$ were obtained.

The range distributions are studied in Fig. 6. It is seen that both ways of simulating polycrystallinity yield the experimental distribution and that amorphous and random distributions agree with each other but differ from experiment. Also included is the simulation in an amorphous material using the experimental correction values $f_n = 0.78$ and $f_e = 1.0$.[39] Further calculations using the *mean* potential yielded very similar results. The time scale presented in Fig. 6 illustrates why this method is

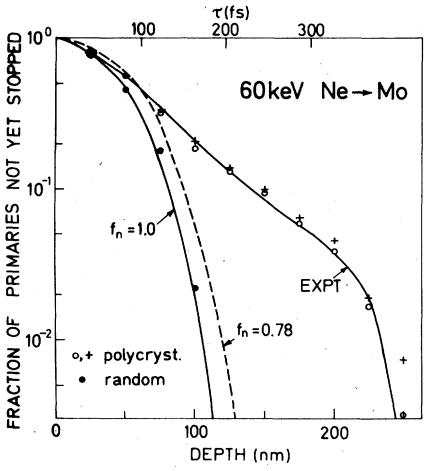

FIG. 6. Integral range distribution of 60-keV Ne in Mo. The experimental curve is reproduced (and deconvoluted) from Ref. 39. In the simulations, the TF potential and LSS electronic stopping was used. The rms vibration amplitude was 0.060 Å. The time per distance scale is calculated using the maximum velocity (6.0×10^5 m/s) of the recoiling nucleus. The target structure was either POLY1 (×), POLY2 (○), random (●), or amorphous, in which case f_n was either 1.0 or 0.78.

usually adequate in the DSA analysis, although the experimental range distribution cannot be produced. In addition, the probability distribution $\exp(-t/\tau)$ of the emission times t causes the short emission times to have more weight than the less frequently occurring longer times in the determination of the $F(\tau)$ value.

In Fig. 7 the $F(\tau)$ curves for the DSA analysis are presented. It is found that polycrystalline and $f_n = 0.78$ curves agree at intermediate τ values, and that the $F(\tau)$ value is sensitive to the initial position of the recoiling ion and to target structure, and so establish limitations on the

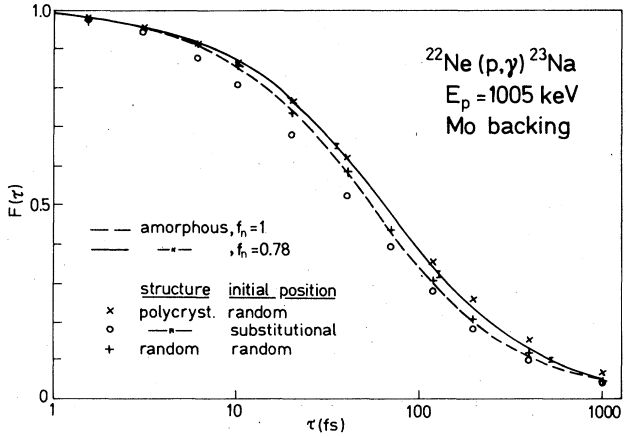

FIG. 7. $F(\tau)$ curves for the reaction ^{22}Ne$(p,\gamma)^{23}$Na, $E_p = 1005$ keV, for amorphous, random, and polycrystalline Mo backing. When the target has crystalline structure, the initial position of the recoiling ion is either substitutional lattice site or random. The error bars are calculated as described in text.

accuracy of the experimentally measured τ values.

In Fig. 8 the line shapes for the experimentally measured $\tau=120$ fs are compared with experiment. It is seen that the polycrystalline line shape agrees well with the experimental one (with 0.81% implanted atoms), whereas the amorphous one with $f_n=0.78$ shows some deviation. Figure 8 shows a typical feature that is introduced by the polycrystallinity, namely, the more varying structure in the line shapes.

As a rule, the calculation should yield an upper limit for the τ value in the analysis of low-dose experiments, because the implanted atoms and the damage both increase the slowing down and thus lower the $F(\tau)$ and τ values. Some calculations were made to study the importance of these factors in the present case. The inclusion of the implanted atoms in the simulations is not straightforward, but the approximative results indicate that 0.81% of the implanted atoms do not have a noticeable effect on the $F(\tau)$ values. On the other hand, if the crystal is randomly rotated, on an average after 100 collisions, the $F(\tau)$ value changed from 0.356 ± 0.006 to 0.345 ± 0.006, and the range distributions closely resembled the $f_n=0.78$ curve in Fig. 6 and the line shapes are in agreement with experiment (Fig. 8).

The results in Figs. 6 and 7 demonstrate clearly that if polycrystallinity is introduced in the calculation, no parameters are needed to get agreement with low-dose experiment and the combined DSA- and range-measurement method should be sensitive and sufficiently accurate to reveal possible diffusional effects in the range distributions.

Usually, the comparison with DSA studies is complicated by the large doses needed to yield good statistics in γ-ray line shapes. However, some further comparisons have been made. 20-, 60-, and 100-keV N-in-Ta range distributions[13] could be reproduced only if some damage was introduced in the polycrystalline material. In the comparison of the calculated $F(\tau)$ values in the $^{13}C(p,\gamma)^{14}N$, $E_p=1150$ keV, reaction in Ta with experimental ones,[40] where a 20% concentration of implanted atoms has been used, good agreement was found if some damage was assumed. For the $^{26}Mg(p,\gamma)^{27}Al$, $E_p=1733$ keV reaction in Ta,[41] good agreement was also found with some damage. These results are in contrast with the range distribution study of 20-, 60-, and 100-keV Al in Ta, where some texture was needed for Ta.[35] A probable explanation is that Al atoms diffuse before they are trapped. This explanation is supported by the calculated 100-keV profile assuming texture, which displayed too long a tail.[35] This is understandable, if diffusion is the explanation. It is energy independent and thus relatively more pronounced at smaller energies. The error in stopping power is not a likely reason, because it would yield an error also in the DSA studies. We showed earlier that the experimental distributions can be reproduced, if diffusion is allowed to change the calculated distributions.[9]

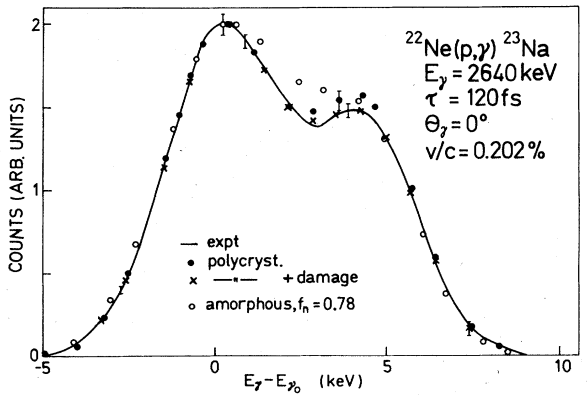

FIG. 8. Line shapes for $\tau=120$ fs at 0° detector angle. They are convoluted by the energy resolution (full width at half maximum=3.4 keV), and in the simulations the finite size of the detector in the experimental measurements (Ref. 39) was taken into account (the solid angle subtended by the detector was 37°). The maximum Ne concentration in the experiment was 0.81 at. %, and in the simulations the target was either amorphous, with $f_n=0.78$ (○), or polycrystalline, with damage (×) or without damage (●). The experimental curve is reproduced from Ref. 39.

IV. DISCUSSION

On the basis of the comparisons made, we may conclude that COSIPO produces the results in agreement with MIM and other BCAM codes in the keV region, although the results become increasingly sensitive to the parameters and the potential at $\epsilon<0.02$. This is the lower limit that Latta gives for ϵ below which the range calculations based on realistic potentials begin to differ.[42] On the other hand, this is the energy region which yields information on the potential and is therefore of importance. In the DSA analysis the typical ϵ value of the recoiling ion is $\epsilon\sim1$, where there is very little difference in nuclear stopping powers calculated from different potentials. The good agreement found between calculations and both DSA and range measurements (Figs. 6–8) is strong indication that the potential is correct and that possible deviations in the slowing down are due to the structure of the target (including implanted atoms, damage, and texture) and diffusion.

On the other hand, at $\epsilon<0.02$ experimental measurements show that the mean ranges of projectiles with different atomic numbers display variations about a curve which is calculated with a semiempirical potential.[43,44] At $\epsilon=0.04$ the oscillations are less than 10%,[43] and at $\epsilon=0.1$ they have disappeared altogether.[43]

The Gordon-Kim method for potentials is in fact appropriate only for ground-state and closed-shell atoms. Neither of these assumptions is usually valid in stopping processes. However, the Gordon-Kim method can be employed here, because the screening in the interatomic potential is mainly due to the inner-shell electrons at shorter distances. Only at $\epsilon<0.04$ can the outer-shell effects and excitations no longer be ignored in calculation stopping. As we have recently shown, statistical calculating which is based on the assumptions that the electron distributions of the interacting atoms are spherically symmetric and undisturbed, do not yield sufficiently large variations in the potential to explain the experimental multiple scattering

data of various ions in xenon targets.[10] It should be noted that the calculated and experimental values agreed in the cases of closed-shell argon and krypton, but diverged strongly in the cases of copper and silver. Consequently, more refined methods are needed at low energies.

In the calculations it has been assumed that the elastic and inelastic parts of the energy loss can be separated. Robinson and Torrens[18] give the equations, where the effect of the inelastic energy loss is included in the elastic scattering calculations. Those equations show that the assumption is well justified. At higher energies the inelastic energy loss plays a major role in stopping. It has been pointed out that for $\epsilon \gtrsim 10$ the calculated backscattering cross section of He ions agrees with experiment to within the experimental accuracy (1%) (e.g., Ref. 45). This again indicates that the elastic and inelastic energy losses can be treated separately.

In conclusion, we maintain that above $\epsilon \gtrsim 0.04$ there remains little interest in nuclear stopping power in itself; if the structure of the target is known, the elastic slowing down of ions can be calculated at least to an accuracy of 10%.[4,5,7,42,43] Thus only the lack of a detailed knowledge of the target structure (and diffusion) makes the measurements necessary in application.

An immediate application of knowing the slowing down is that it should be possible to improve the accuracy of the DSA measurements at low (~ 10 fs) and high (~ 1000 fs) τ values, where the uncertainty in the $F(\tau)$ curves is largest and the experimental correction procedure least accurate, or at least the τ values should be put on a more firm basis by these means.

In normal cases, where large implant doses are needed for good statistics in the DSA measurements, there is less help from the present method, and an individual study of target structure must be made, as in Ref. 39. Then, the crystalline structure effects are small as well. If the only purpose of the measurement is the lifetime values, it should even be possible to include the effect of the crystalline structure on slowing down as a correction factor in the Blaugrund method in the way described by Latta.[46] At least the upper limit for the τ value could be calculated this way, if there is no change in the density of the backing (for density effects, see Refs. 39 and 41).

We may invert the above situation; thus, when the nuclear stopping is known, we may, by DSA measurements, study the structure of the target and the initial position of the implanted atoms, as absolute $F(\tau)$ values and γ-ray line shapes are sensitive to these factors (Figs. 7 and 8).

It can be seen from Fig. 7 that the "effective" nuclear stopping is about 20% *smaller* (i.e., $f_n = 0.8$) in a polycrystal than in an amorphous material. However, if the initial position of the recoiling Ne atom considered is a substitutional lattice site, the effective nuclear stopping is about 20% larger (f_n would be 1.2). The difference in the $F(\tau)$ values is about 20% between the cases where the initial position of the recoiling ion is either substitutional or interstitial (by comparison, the difference between the results for an initial position either random or interstitial is small). In favorable cases the $F(\tau)$ value can be measured to an accuracy of at least 3%.[39] This means that it should even be possible to measure the percentage of the atoms in substitutional lattice sites. In metallurgy an important problem is to determine the lattice locations of nitrogen and boron atoms in various kinds of steel. The method presented above should be sensitive enough for this purpose. When the structure of the target is known (e.g., by DSA measurements) it should also be possible to study diffusion during implantation by experimentally measuring the concentration profiles of implanted ions. Some experiments are planned to study whether or not the method is sufficiently sensitive to be used in such applications.

[1] W. D. Wilson and C. L. Bisson, Phys. Rev. B **8**, 3984 (1971).
[2] P. T. Wedepohl, Proc. Phys. Soc. London **92**, 79 (1967).
[3] P. Gombas, *Statistical Theory of Atoms* (Springer, Vienna, 1949).
[4] W. D. Wilson, L. G. Haggmark, and J. P. Biersack, Phys. Rev. B **15**, 2458 (1977).
[5] M. Bister, M. Hautala, and M. Jäntti, Radiat. Eff. **42**, 201 (1979).
[6] R. S. Gordon and Y.S . Kim, J. Chem. Phys. **56**, 3122 (1972).
[7] M. Hautala and M. Bister, Radiat. Eff. **54**, 191 (1981).
[8] M. Hautala, R. Paltemaa, A. Anttila, and M. Luomajärvi, Nucl. Instrum. Methods **209-210**, 37 (1983).
[9] M. Hautala, Radiat. Eff. **51**, 35 (1980).
[10] A. Luukkainen, M. Hautala, and M. Bister, Nucl. Instrum. Methods B **2**, 173 (1984).
[11] M. Bister, J. Keinonen, and A. Anttila, Phys. Lett. **74A**, 357 (1979).
[12] J. Keinonen, M. Hautala, M. Luomajärvi, A. Anttila, and M. Bister, Radiat. Eff. **39**, 189 (1978).
[13] M. Luomajärvi, J. Keinonen, M. Bister, and A. Anttila, Phys. Rev. B **18**, 4657 (1978).
[14] W. L. Gay and D. E. Harrison, Phys. Rev. **135**, A1780 (1964).
[15] H. Lutz, R. Schuckert, and R. Sizmann, Nucl. Instrum. Methods **38**, 241 (1965).
[16] J. B. Gibson, A. N. Goland, M. Milgram, and G. H. Vineyard, Phys. Rev. **120**, 1229 (1960).
[17] M. T. Robinson and O. S. Oen, Phys. Rev. **132**, 2385 (1963).
[18] M. T. Robinson and I. M. Torrens, Phys. Rev. B **9**, 5008 (1974).
[19] M. Hou and M. T. Robinson, Nucl. Instrum. Methods **132**, 641 (1976).
[20] D. E. Harrison, Radiat. Eff. **70**, 1 (1983).
[21] M. T. Robinson, in *Sputtering by Particle Bombardment II,* edited by R. Behrisch (Springer, New York, 1981).
[22] *Channeling,* edited by D. V. Morgan (Wiley, London, 1973).
[23] D. E. Harrison, R. W. Leeds, and W. L. Gay, J. Appl. Phys. **36**, 3154 (1965).
[24] J. F. Ziegler, J. P. Biersack, and U. Littmark, in Proceedings of the International Ion Engineering Congress, edited by H. T. Takagi (Institute of Electrical Engineers of Japan, Tokyo,

1983), p. 1861.
[25]B. M. Latta, Can. J. Phys. **58**, 1783 (1980).
[26]D. E. Harrison and D. S. Greiling, J. Appl. Phys. **38**, 3200 (1967).
[27]E. V. Kornelsen, F. Brown, J. A. Davies, and G. R. Piercy, Phys. Rev. **136**, A849 (1964).
[28]B. M. Latta and P. J. Scanlon, Phys. Rev. A **10**, 1638 (1974).
[29]J. Lindhard, M. Schraff, and H. E. Schiøtt, Mat. Fys. Medd. Dan. Vid. Selsk. **33**, no. 14 (1963); J. Lindhard, V. Nielsen, and M. Scharff, Mat. Fys. Medd. Dan. Vid. Selsk. **36**, no. 10 (1968).
[30]O. B. Firsov, Zh. Eksp. Teor. Fiz. **36**, 1517 (1959) [Sov. Phys.—JETP **9**, 1076 (1959)].
[31]W. M. Currie, Nucl. Instrum. Methods **73**, 173 (1969).
[32]L. Eriksson, J. A. Davies, and P. Jespergård, Phys. Rev. **161**, 219 (1967).
[33]M. Hautala, Nucl. Instrum. Methods B **2**, 130 (1984).
[34]W. Möller and W. Eckstein, Nucl. Instrum. Methods **194**, 121 (1982).
[35]M. Hautala, Phys. Lett. **95A**, 436 (1983).
[36]D. P. Jackson and J. H. Barrett, Comput. Phys. Commun. **13**, 157 (1977).
[37]J. A. Davies, L. Eriksson, and J. L. Whitton, Can. J. Phys. **46**, 573 (1968).
[38]M. Hautala, Nucl. Instrum. Methods B **2**, 799 (1983).
[39]J. Keinonen, A. Luukkainen, A. Anttila, and M. Erola, Nucl. Instrum. Methods **216**, 249 (1983).
[40]M. Bister, A. Anttila, and J. Keinonen, Phys. Rev. C **16**, 1303 (1977).
[41]A. Anttila, M. Bister, A. Luukkainen, A. Z. Kiss, and E. Somorjai, Nucl. Phys. Sect. A **385**, 194 (1982).
[42]B. M. Latta, Can. J. Phys. **58**, 1738 (1980).
[43]F. Besenbacher, J. Bøttiger, T. Larssen, P. Loftager, and W. Möller, Nucl. Instrum. Methods **178**, 517 (1980).
[44]J. Berthold and S. Kalbitzer, Nucl. Instrum. Methods **209-210**, 13 (1983).
[45]M. Hautala and M. Luomajärvi, Radiat. Eff. **45**, 159 (1980).
[46]B. M. Latta, in *Proceedings of the 10th International Conference on Atomic Collisions in Solids, Bad Iburg, West Germany, 1983* (unpublished).